

# Stereoelectronic, Vibrational, and Environmental Contributions to Polarizabilities of Large Molecular Systems: A Feasible Anharmonic Protocol

Franco Egidi,<sup>\*,†</sup> Tommaso Giovannini,<sup>†</sup> Matteo Piccardo,<sup>†</sup> Julien Bloino,<sup>†,‡</sup> Chiara Cappelli,<sup>§</sup> and Vincenzo Barone<sup>†</sup>

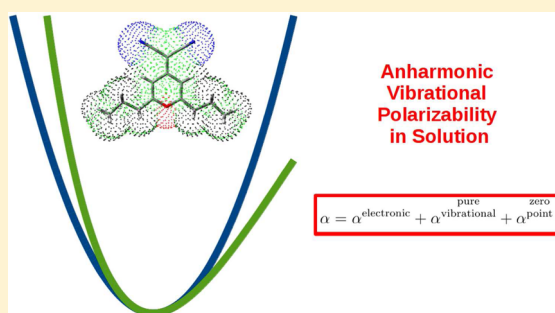
<sup>†</sup>Scuola Normale Superiore, Piazza dei Cavalieri 7, 56126 Pisa, Italy

<sup>‡</sup>Consiglio Nazionale delle Ricerche, Istituto di Chimica dei Composti Organometallici, UOS di Pisa, Via G. Moruzzi 1, 56124 Pisa, Italy

<sup>§</sup>Dipartimento di Chimica e Chimica Industriale, Università di Pisa, via Risorgimento 35, 56126 Pisa, Italy

## Supporting Information

**ABSTRACT:** Reliable computations of linear and nonlinear optical properties of molecular systems in condensed phases require a proper account of stereoelectronic, vibrational, and environmental effects. In the framework of density functional theory, these effects can be accurately introduced using second-order vibrational perturbation theory in conjunction with polarizable continuum models. We illustrate the combination of an anharmonic description of the ground-state potential energy surface with solvation effects treated with the polarizable continuum model (PCM) in the calculation of the electronic, zero-point, and pure vibrational polarizabilities of selected systems. The description of the solvation environment is enriched by taking into account the dynamical aspects of the solute–solvent interactions through the inclusion of both electronic and vibrational nonequilibrium effects, as well as the direct effect of the solvent on the electric field that generates the molecular response (local field effect). This treatment yields accurate results which can be directly compared with experimental findings without the need of empirical corrections.



## 1. INTRODUCTION

Linear and nonlinear optical properties, especially (hyper)polarizabilities, of molecular systems are of remarkable and increasing interest in a number of research fields, on both a fundamental and a technological level.<sup>1–3</sup> In this context, the role of quantum mechanical approaches for complementing experimental studies is continuously increasing from both the point of view of the dimensions of the systems amenable to accurate computations and the point of view of the inclusion of dynamic and environmental effects in addition to intrinsic stereoelectronic ones. Even pending further developments for specific shortcomings, latest-generation density functionals are providing sufficiently reliable results for the nonlinear properties of isolated molecules at their equilibrium geometries<sup>4</sup> to warrant consideration of additional effects. As a matter of fact, a number of studies have demonstrated the importance of both vibrational and environmental contributions to (hyper)polarizabilities.<sup>5–8</sup> These contributions can in many cases be significant and in some circumstances (especially for the static case) even dominate over the electronic equilibrium value of the isolated system ( $\alpha^{\text{eq}}$ ). Among the various terms, the zero-point contribution ( $\Delta_{\text{zp}}\alpha$ ) arises from harmonic and/or anharmonic nuclear oscillations around the equilibrium geometry. This term is equivalent to vibrational averaging

effects on other electronic properties<sup>9–12</sup> and can be computed once first and second derivatives of polarizability with respect to geometric parameters are available. Next, the pure vibrational contributions ( $\alpha^{\text{v}}$ ), including both harmonic and anharmonic terms, arise from excitations within the vibrational manifold of the electronic ground state, rather than the electronic excited states, as is the case for the electronic contributions to the (hyper)polarizabilities. Depending on the specificity of the system under study and the experimental conditions that one is set to reproduce with the chosen theoretical model, some, or even all, of these effects may be needed to achieve the desired accuracy. Finally, proper treatment of environmental effects, even in the context of continuum methods (i.e., in the absence of specific system–environment interactions) requires implementations going well beyond standard models and including nonequilibrium and local field effects. Following previous work in our group we have now implemented these terms in the general anharmonic model sketched above. This allows the proper consideration of all the dominant effects and the disentanglement of their relative contribution to the overall experimental outcome. In this first report, we will be concerned

**Received:** March 12, 2014

with polarizabilities (both static and frequency-dependent) only, whereas hyperpolarizabilities will be dealt with in forthcoming studies. After a short presentation of the essential physical-mathematical background and of implementation and computational details, we will discuss specific examples in order to illustrate the possibilities and the reliability of this computational tool. The general aim is to show that, apart from the specific interest of the studied systems, a robust and user-friendly computational tool is now available for complementing experimental analyses.

## 2. THEORY

**2.1. The Molecular Polarizability.** Within the Born–Oppenheimer approximation, the molecular polarizability (both static and frequency-dependent) can be written as the sum of three terms:<sup>13,14</sup>

$$\alpha = \alpha^{\text{eq}} + \Delta_{\text{zp}}\alpha + \alpha^{\text{v}} \quad (1)$$

The first term denotes the electronic polarizability of the molecule at the equilibrium geometry. The second term is its zero-point vibrational correction, and the last term is the pure vibrational polarizability. When computing the two vibrational contributions, we assume that only the ground vibrational state is populated. The electronic term, which can be computed by means of response theory with most electronic structure methods, is expected to be the most important of the three, both in the frequency-dependent case and in the static limit. Previous studies however have pointed out that in order to obtain accurate results, the effect of molecular vibrations should not be ignored.<sup>5–7</sup> The two vibrational terms in eq 1 are of a very different nature. The pure vibrational polarizability can be related to the change of the electric dipole moment as the molecule vibrates and can be expressed as a sum-over-states:<sup>15,16</sup>

$$\alpha_{\alpha\beta}^{\text{v}} = \frac{2}{\hbar} \sum_{w \neq 0} \frac{\omega_{w0}}{\omega_{w0}^2 - \omega^2} \langle 0 | \mu_{\alpha} | w \rangle \langle w | \mu_{\beta} | 0 \rangle \quad (2)$$

where  $\mu$  is the electric dipole moment,  $\omega_{w0}$  is the difference between the energy of state  $w$  and the ground-state energy,  $\omega$  is the angular frequency of the electric field,  $|0\rangle$  is the ground vibrational state of the molecule, and the summation runs over all other vibrational states belonging to the same electronic level. It is clear from this expression that, as  $\omega$  increases, the pure vibrational contribution goes to zero; it is therefore expected to be negligible in the case of light in the UV–visible range of the spectrum. This term can instead be significant in the case of the static polarizability. The zero-point correction to the electronic polarizability stems from the fact that the latter is computed for the molecule at the equilibrium geometry, but even at zero absolute temperature the nuclei cannot be considered fixed. Any electronic property, such as the electronic polarizability, can thus be averaged using the vibrational wave function of the system, giving rise to the remaining terms of eq 1. Contrary to the pure vibrational term, the vibrational correction can give a significant contribution both in the static and in the frequency-dependent case. The calculation of the vibrational terms requires a model for the potential energy surface (PES) of the system. The harmonic approximation is usually invoked in this case, where the electrostatic potential is expanded up to the second order, giving a description of the molecular vibrations in terms of normal modes. The harmonic approximation however may not be accurate enough to provide

an adequate description of the system, and inclusion of anharmonicity effects has been shown to be crucial in the modeling of electronic properties<sup>10–12</sup>

In the case of the static polarizability, an additional term is usually included: a static electric field causes molecules with a nonzero dipole moment to partially reorient along the field axis,<sup>17</sup> so a direct experimental measurement of the static polarizability of a system naturally includes a term which depends on the dipole moment of the system and the temperature. This term, denoted in the following by  $\alpha_{\mu}$ , is equal to  $|\mu|^2/3k_{\text{B}}T$  for a molecular system in the gas phase. This quantity should be added to the computed static polarizability before any meaningful comparison with experimental findings is made.

**2.2. Anharmonicity Effects on the Polarizability.** In this work, we model the anharmonicity of the PES using our implementation<sup>18–21</sup> of second-order vibrational perturbation theory (VPT2) which is able to provide an accurate description of both anharmonic vibrational energies and wave functions. Within the framework of perturbation theory, it is also useful to expand electronic properties which depend on the molecular geometry, such as the dipole moment or the electronic polarizability, in a Taylor series around the equilibrium structure and truncate the expansion at the required order. Usually, one only keeps the lowest-order that gives a nonzero contribution if combined with the harmonic vibrational wave function. However, if anharmonicity effects are introduced, the effects of the so-called electric anharmonicity (i.e., contributions from higher-order terms in the electronic property expansions) should also be considered. In the case of electronic properties we are considering here, the anharmonic wave function obtained via VPT2 can be combined with the Taylor expansions of the electric dipole moment and electronic polarizability to rewrite the previous equations, giving explicit expressions for both the vibrational average and the anharmonic pure vibrational polarizability. The vibrational average results in two terms, the first one accounting for the mechanical anharmonicity, and the second term accounting for the electric anharmonicity. This separation is denoted by the indices in the apex, the first one denoting the level of electric anharmonicity and the second one denoting the level of mechanical anharmonicity:<sup>13,14</sup>

$$\begin{aligned} \Delta_{\text{zp}}\alpha &= -\frac{\hbar}{4} \sum_a \frac{1}{\omega_a^2} \left( \frac{\partial \alpha}{\partial Q_a} \right) \sum_b \frac{K_{abb}}{\omega_b} + \frac{\hbar}{4} \sum_a \frac{1}{\omega_a} \left( \frac{\partial^2 \alpha}{\partial Q_a^2} \right) \\ &= [\alpha]^{0,1} + [\alpha]^{1,0} \end{aligned} \quad (3)$$

The pure vibrational terms can be treated in a similar way obtaining explicit formulas that depend on the derivatives of the electric dipole moment, in addition to the cubic and quartic force constants. The total value is separated into a harmonic term and three anharmonic contributions which are distinguished according to their degree of mechanical and electric anharmonicity:

$$\alpha^{\text{v}} = [\mu^2]^{0,0} + [\mu^2]^{0,2} + [\mu^2]^{1,1} + [\mu^2]^{2,0} \quad (4)$$

We compute these terms using the formulas obtained by Bishop et al.,<sup>13–16</sup> albeit with a slightly different expression for the  $[\mu^2]^{0,2}$  term, shown in the Appendix, since we found the original expression for this term reported in the literature to be incorrect. Anharmonic calculations tend to be very expensive for medium to large sized systems because they require the

evaluation of force constants up to the fourth order, as well as high-order geometrical derivatives of the electronic properties under investigation. If the harmonic frequencies can be computed analytically, all the required anharmonic terms (i.e., all third derivatives and fourth derivatives with up to three different indices) can be found by numerical differentiation of lower-order terms by displacing the atoms along each normal mode both in the positive and in the negative directions. This number of separate calculations that must be performed scales with system size; therefore particular care should be taken in the case of larger systems.

### 2.3. The Molecular Polarizability of Solvated Systems.

Polarizabilities and hyperpolarizabilities describe a system's response to an external static or dynamic electric field. If the system under consideration is a solution, the mutual interactions between the solvent, solute, and the electromagnetic field should all be considered in determining the system's response. Even in the absence of external radiation, a solvent induces profound changes in solute molecules: the electron density, ground-state geometry, and conformational distribution are all affected, and these changes are reflected in all molecular properties, including response properties. When considering electric-field induced responses, in addition to the effect on the solute, the effect of the solvent on the field itself should be considered.<sup>22</sup> The solute's response is caused by the field locally acting on it, which is different than the external field because of the solvent's screening effect. Traditionally the problem is addressed via the Onsager–Lorentz model,<sup>24</sup> which is based on the assumption that the molecule can be treated as a point-like electric dipole at the center of a spherical cavity within a polarizable continuum, the latter representing the solvent. The local field can then be related to the external field through a simple multiplicative factor which only depends on the solvent's static dielectric constant ( $\epsilon$ ) for static fields ( $\vec{E}^{\text{loc}}$ ), and on the solvent's optical dielectric constant ( $\epsilon_{\text{opt}}$ ) for dynamic fields ( $\vec{E}_{\omega}^{\text{loc}}$ ):

$$\vec{E}^{\text{loc}} = \frac{\epsilon + 2}{3} \vec{E}^{\text{ext}}; \quad \vec{E}_{\omega}^{\text{loc}} = \frac{\epsilon_{\text{opt}} + 2}{3} \vec{E}_{\omega}^{\text{ext}} \quad (5)$$

The Onsager–Lorentz model has often been used in reverse, to estimate a molecule's gas-phase polarizability and hyperpolarizabilities from experimental data measured in solution. This model is, however, very crude, as it only reduces the solute's electron density to the sole dipole term, and assumes a spherical cavity regardless of the molecular shape. Notably, the computed factors are the same for every solute as they only depend on the solvent's dielectric properties.

In this work, we treat solvation effects by means of the polarizable continuum model (PCM),<sup>25,26</sup> which treats the solvent as a polarizable continuum with given dielectric properties. The molecule, treated quantum-mechanically, is placed inside of a molecule-shaped cavity carved within the polarizable continuum, and a mutual polarization between the solute's electronic density and the dielectric continuum is established. The solvent's polarization affects the solute through appropriate terms that are added to the Hamiltonian, which can be carried over to molecular property calculations, including response properties. PCM, therefore, can treat both the “direct” solvent effect on the electronic density and the “indirect” effect on the molecular geometry. PCM can also be used to integrate local-field effects in the calculation in a more accurate way than the Onsager–Lorentz model, by introducing the concept of “effective” molecular response properties, which directly

describe the response of the solute to the external field in the liquid.<sup>27</sup> As in the Onsager–Lorentz model, local field effects on the static (hyper)polarizabilities are computed using the solvent's static dielectric constant, whereas their dynamical counterparts are computed using the optical dielectric constant (i.e., the square of the refractive index). Note that the sum-over-state expression for the polarization  $P$  in the case of a general first-order process can be written as follows:<sup>28</sup>

$$P_{\omega} = -\frac{1}{\hbar} \sum_{m \neq n} \left( \frac{\langle n | \hat{\mu} | m \rangle \langle m | \hat{V}_{\omega} | n \rangle}{\omega_{mn} - \omega} + \frac{\langle n | \hat{V}_{\omega} | m \rangle \langle m | \hat{\mu} | n \rangle}{\omega_{mn}^{*} + \omega} \right) \quad (6)$$

In the case of the electronic polarizability of a system in the gas phase we have  $\hat{V}_{\omega} = -\vec{\mu} \cdot \vec{E}_{\omega}$ . In the condensed phase, we should use the local field  $\vec{E}_{\text{loc}}$  instead of the external field. Alternatively, as already mentioned above, we may consider the external field acting on an effective dipole moment  $\mu^{\text{eff}}$ , which, in the PCM framework, can be easily computed as a sum of the dipole moment of the solvated molecule and a contribution due to the charge density induced by the molecule on the cavity surface. The effective dipole moment replaces the molecular dipole moment in the  $\hat{V}_{\omega}$  term only; therefore calculations including local-field effects must be done with care, using the two different dipole moments where appropriate.<sup>29</sup>

In the case of response properties induced by time-dependent fields, additional solvent effects, related to the dynamical aspects of solvation, should be considered. Dynamical polarizabilities and hyperpolarizabilities describe a system response to oscillating fields, usually in the visible range of the spectrum. The solute's electronic density evolves in time according to the characteristic time-scale of the perturbation, and while some degrees of freedom of the solvent are able to instantaneously rearrange to the new solute electronic density, others remain static, entering a nonequilibrium configuration. For visible light, it can be assumed that only the electrons of the solvent molecules will be able to rearrange themselves to the oscillating solute electronic density, while the nuclei will remain fixed. This effect is included in the calculation of the electronic component of optical rotation within the PCM framework by separating the solvent polarization into two different contributions,<sup>30</sup> one accounting for the “fast” degrees of freedom of the solvent, and one induced by the “slow” degrees of freedom, responsible for the nonequilibrium effect. This electronic nonequilibrium effect does not apply to the case of static polarizabilities.

### 2.4. Combining Solvation and Vibrational Effects.

Solvent effects described so far apply to the calculation of the electronic polarizability; however, the focus of this work is the modeling of vibrational effects on polarizabilities of solvated systems. The presence of a solvent alters the PES of the solute molecules, with repercussions on all vibrational properties, including vibrational frequencies,<sup>31,32</sup> infrared (IR) and vibrational circular dichroism (VCD) spectroscopic intensities,<sup>33,34</sup> and, of course, pure vibrational components and vibrational averages of electronic properties. PCM can be effectively used to include these effects in ab initio calculations; however, special care should be taken when considering the appropriate solvation regime to be adopted. The solute's vibrational motion causes an additional nonequilibrium polarization in the solvent because its translational and rotational degrees of freedom cannot evolve within the time-scale characteristic of a molecular vibration. As in the case of electronic nonequilibrium, in PCM a



separate set of polarization charges can be defined to account for the nonequilibrium polarization. The free-energy of the system can thus be rewritten and differentiated to yield the nonequilibrium vibrational wave function and vibrational frequencies. This treatment can also be extended to the calculation of the anharmonic force field, and to the geometrical derivatives of all molecular properties. In the case of (hyper)polarizabilities, we require the property first and diagonal second derivatives with respect to the normal modes to compute the vibrational correction, and also the derivatives of the dipole moment to compute the pure vibrational contributions. Note that all quantities are computed with the inclusion of local field effects and, in the case of dynamical (hyper)polarizabilities, electronic nonequilibrium effects. For example, the harmonic contribution to the pure vibrational polarizability becomes<sup>8</sup>

$$[\mu^2]_{\omega}^{0,0} = \sum_a \frac{\partial \mu_a}{\partial \bar{Q}_a} \frac{\partial \mu_{\beta}^{\text{eff}}}{\partial \bar{Q}_a} \bar{\lambda}_a \quad (7)$$

where the summation runs over all normal modes,  $\lambda_a = (\omega_a^2 - \omega^2)^{-1}$ , and all quantities bearing an overline are computed in the vibrational nonequilibrium regime. Anharmonic contributions and the zero point correction can also be treated in a similar way.

This approach yields physically consistent quantities that can be directly compared with experimental data, which no longer need to be empirically corrected to estimate the solvent's contributions.

### 3. COMPUTATIONAL DETAILS

All calculations were performed using a locally modified version of the Gaussian09 quantum chemistry suite of programs.<sup>35</sup> The CAM-B3LYP<sup>36</sup> functional was used for all systems since it has been reported to yield reliable results for both the electronic and pure vibrational polarizability.<sup>4,37,38</sup> Different functionals were also tested, including B3LYP,<sup>39,40</sup> M06-2X,<sup>41</sup> PBE0,<sup>42</sup> and  $\omega$ B97X,<sup>43</sup> with consistent results, reported in the Supporting Information, showing the computed property to be rather robust with respect to the change of functional, especially for the long-range corrected CAM-B3LYP and  $\omega$ B97X, which are particularly appropriate for the push–pull systems here analyzed.

The considered systems are shown in Figures 1 and 3. For all calculations concerning pNA and dNA we used the aug-cc-pVDZ<sup>44</sup> basis set, whereas we employed the 6-31+G\* basis set for DPDCP and the bichromophoric system in Figure 3. Solvent effects were accounted for using PCM,<sup>25,26</sup> with the addition of local field and nonequilibrium effects. Molecular cavities were built using a set of interlocking spheres centered on the atoms, with radii according to the Gaussian 09 defaults. The solvents' static and optical dielectric constants used are  $\epsilon = 2.27$  and  $\epsilon_{\text{opt}} = 2.25$  for benzene,  $\epsilon = 2.23$  and  $\epsilon_{\text{opt}} = 2.13$  for  $\text{CCl}_4$ , and  $\epsilon_0 = 2.21$  and  $\epsilon_{\text{opt}} = 2.02$  for 1,4-dioxane. In the following tables, we report the isotropic polarizabilities (the trace of the polarizability tensor divided by 3)  $\alpha_{\text{is}}$ , as well as the longitudinal component (along the molecular axis)  $\alpha_{zz}$ . All polarizabilities are reported in  $\text{cm}^3 \text{mol}^{-1}$ , and all solution values include local field effects and are computed in the vibrational nonequilibrium regime, unless otherwise stated.

### 4. NUMERICAL RESULTS

Para-nitroaniline (pNA, Figure 1a) is a prototypical push–pull system whose linear and nonlinear optical properties have

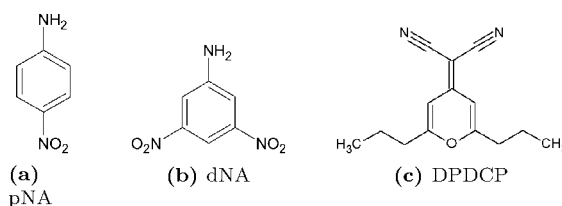


**Figure 1.** Structures of the first three systems studied.

received much attention in the literature, both theoretically and experimentally, and previous results allow us to test the model and make useful comparisons.<sup>45–51</sup> We optimized the geometry of the molecule in the  $C_{2v}$  symmetry. This geometry however results in a vibrational mode with an imaginary frequency with modulus  $238 \text{ cm}^{-1}$ , meaning it is actually a saddle point. The incriminated mode is the umbrella motion of the aminic group, so the lowest-energy geometry would have a  $C_s$  symmetry and a pyramidalized  $\text{NH}_2$  group. We computed the energy profile for the umbrella motion and found that the energy barrier is very low (about  $50 \text{ cm}^{-1}$ ), too low to support a single vibrational mode. At the present time, we lack a rigorous treatment for double-well potentials, though some approaches have been proposed;<sup>52–54</sup> therefore we preferred to perform all calculations on the  $C_{2v}$  structure, which is surely more representative than the  $C_s$  one, and discard the contribution of the imaginary frequency mode to the pure vibrational and zero-point contributions. Figure 2 shows the contribution of each normal mode (except the imaginary frequency one) to the zero-point and harmonic pure vibrational static polarizability of pNA in vacuo. It must be emphasized that the two contributions are unrelated since the first is computed from the polarizability derivatives while the second depends on the dipole derivatives. For a  $C_{2v}$  molecule such as pNA, this implies that they obey different symmetry rules; e.g.,  $a_2$  modes give a vanishing pure vibrational polarizability, but they contribute to the  $[\alpha]^{1,0}$  term in the zero-point polarizability, while the  $[\alpha]^{0,1}$  term originates solely from the total symmetric modes. The greatest contribution to the pure vibrational polarizability comes from mode 30 (a symmetric N–O stretching), followed by modes 25 and 36, which are symmetric bending motions of the hydrogen atoms (see the Supporting Information for a graphical representation of the modes mentioned in the article), while modes 19 and 30 contribute the most to the zero-point polarizability. While some modes give particularly high contributions, it is not possible to discard some of them *a priori* with the aim of reducing the computational cost, as the contributions from other modes add up to give non-negligible values. A similar conclusion was previously reached in the case of different molecular properties, including magnetic and mixed electric–magnetic properties.<sup>11,12</sup>

Table 1 reports the computed static polarizability of pNA in the gas phase and in 1,4-dioxane solution. To better decouple the different solvation effects considered here, we also report the values computed in a vibrational equilibrium regime, along with the vibrational nonequilibrium values computed with and without the inclusion of cavity field effects. Solvent effects cause a significant change to the computed polarizability at both the electronic and vibrational level, with some of the computed

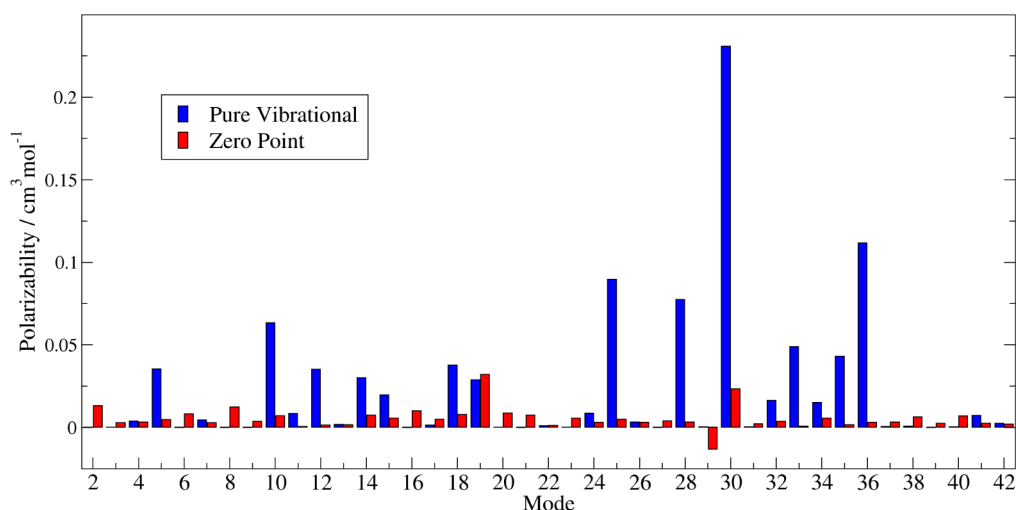


**Figure 2.** Contribution of each normal mode to the zero-point (red) and harmonic pure vibrational (blue) static polarizability of pNA in vacuo.

**Table 1. Static Polarizability of pNA in Vacuo and 1,4-Dioxane Solution<sup>a</sup>**

|                   |               | $\alpha^{\text{eq}}$ | $[\alpha]^{1,0}$ | $[\alpha]^{0,1}$ | $[\mu^2]^{0,0}$ | $[\mu^2]^{2,0}$ | $[\mu^2]^{1,1}$ | $[\mu^2]^{0,2}$ | $\alpha_{\mu}$ | $\alpha_{\text{tot}}$ | $\alpha_{\text{exp}}^{55}$ |
|-------------------|---------------|----------------------|------------------|------------------|-----------------|-----------------|-----------------|-----------------|----------------|-----------------------|----------------------------|
| gas               | $\alpha_{zz}$ | 13.650               | 0.197            | 0.094            | 1.861           | 0.011           | −0.057          | 0.942           | 266.2          | 282.9                 |                            |
|                   | $\alpha_{is}$ | 9.206                | 0.149            | 0.061            | 0.931           | −0.001          | −0.024          | 0.112           | 266.2          | 276.6                 |                            |
| sol, vib eq       | $\alpha_{zz}$ | 16.597               | 0.282            | 0.131            | 3.063           | 0.003           | −0.017          | −0.552          | 362.3          | 381.8                 |                            |
|                   | $\alpha_{is}$ | 10.833               | 0.199            | 0.079            | 1.425           | −0.003          | −0.006          | −0.392          | 362.3          | 374.4                 |                            |
| sol, vib neq      | $\alpha_{zz}$ | 16.604               | 0.256            | 0.140            | 3.001           | −0.001          | −0.016          | −0.212          | 362.1          | 381.9                 |                            |
|                   | $\alpha_{is}$ | 10.837               | 0.193            | 0.085            | 1.430           | −0.005          | −0.007          | 0.041           | 362.1          | 374.7                 |                            |
| sol, vib neq + lf | $\alpha_{zz}$ | 18.342               | 0.281            | 0.156            | 3.285           | −0.001          | −0.047          | −0.201          | 401.2          | 423.0                 |                            |
|                   | $\alpha_{is}$ | 12.781               | 0.224            | 0.099            | 1.647           | −0.002          | −0.021          | 0.039           | 401.2          | 416.0                 | 404 ± 6                    |

<sup>a</sup>The solution values are shown in the vibrational equilibrium regime (sol, vib eq), vibrational nonequilibrium (sol, vib neq), and vibrational nonequilibrium with the addition of local field effects (sol, vib neq + lf).

components of the pure vibrational contribution even showing a change of sign, which is particularly noticeable in the case of  $[\mu^2]_{zz}^{0,2}$ , the term that originates from the mechanical anharmonicity. Switching to a vibrational nonequilibrium regime causes a change in all computed contributions; the electronic component changes because of the slight change in equilibrium geometry (which is reoptimized with a fixed PCM cavity), and a much more significant effect is observed in the case of the pure vibrational part, particularly for the term which includes mechanical anharmonicity to second order. Overall the vibrational nonequilibrium effect does not cause significant changes to the computed polarizability in this particular case, owing to the fact that the chosen solvent's static and optical dielectric constants are very similar ( $\epsilon_0 = 2.21$  and  $\epsilon_{\infty} = 2.02$ ); however this might not hold for different systems or different solvents: we performed a test calculation on the same molecule in acetonitrile ( $\epsilon_0 = 35.69$  and  $\epsilon_{\infty} = 1.81$ ) and discovered that the pure vibrational contribution changes by 8% when going from vibrational equilibrium to nonequilibrium (data reported in the Supporting Information). A much greater change is observed when local field effects are included in the calculation. Even though 1,4-dioxane does not have a particularly high polarity, it still perturbs the field experienced by the system quite significantly, affecting all contributions to the polarizability.

Overall, the vibrational contributions account for about 15% of the electronic polarizability, with the greatest contribution originating from the harmonic pure vibrational term. We also obtain an orientational contribution (originating from the

nonzero dipole moment) of  $401.2 \text{ cm}^3 \text{ mol}^{-1}$ , which makes the total computed static polarizability equal to  $416.0 \text{ cm}^3 \text{ mol}^{-1}$ . This is to be compared with the value of  $404 \pm 6 \text{ cm}^3 \text{ mol}^{-1}$  measured by Wortmann et al.,<sup>55</sup> which means that there is a mere 3% discrepancy between theory and experiment. Of course, in this case the greatest contribution is by far the orientational one, which only depends on the dipole moment, so a more meaningful comparison should be done when the former contribution is absent. We therefore computed the frequency-dependent polarizability at 589 nm, in vacuo and in solution (Table 2). We do not report the pure vibrational component because it is negligible for the considered

**Table 2. Dynamic Polarizability of pNA in Vacuo and 1,4-Dioxane Solution Computed for a 589 nm Wavelength<sup>a</sup>**

|                   |               | $\alpha_{\omega}^{\text{eq}}$ | $[\alpha]_{\omega}^{1,0}$ | $[\alpha]_{\omega}^{0,1}$ | $\alpha_{\text{tot}}$ | $\alpha_{\text{exp}}^{55}$ |
|-------------------|---------------|-------------------------------|---------------------------|---------------------------|-----------------------|----------------------------|
| gas               | $\alpha_{zz}$ | 15.29                         | 0.28                      | 0.12                      | 15.69                 |                            |
|                   | $\alpha_{is}$ | 9.91                          | 0.19                      | 0.07                      | 10.17                 |                            |
| sol, vib eq       | $\alpha_{zz}$ | 19.09                         | 0.45                      | 0.19                      | 19.73                 |                            |
|                   | $\alpha_{is}$ | 11.80                         | 0.27                      | 0.10                      | 12.17                 |                            |
| sol, vib neq      | $\alpha_{zz}$ | 19.10                         | 0.41                      | 0.20                      | 19.71                 |                            |
|                   | $\alpha_{is}$ | 11.81                         | 0.25                      | 0.11                      | 12.17                 |                            |
| sol, vib neq + lf | $\alpha_{zz}$ | 20.91                         | 0.45                      | 0.22                      | 21.58                 |                            |
|                   | $\alpha_{is}$ | 13.67                         | 0.29                      | 0.12                      | 14.08                 | 14.1 ± 0.4                 |

<sup>a</sup>The solution values are shown in the vibrational equilibrium regime (sol, vib eq), vibrational nonequilibrium (sol, vib neq), and vibrational nonequilibrium with the addition of local field effects (sol, vib neq + lf).

Table 3. Static Polarizability of dNA in Vacuo and 1,4-Dioxane Solution

|     |               | $\alpha^{\text{eq}}$ | $[\alpha]^{1,0}$ | $[\alpha]^{0,1}$ | $[\mu^2]^{0,0}$ | $[\mu^2]^{2,0}$ | $[\mu^2]^{1,1}$ | $[\mu^2]^{0,2}$ | $\alpha_{\mu}$ | $\alpha_{\text{tot}}$ | $\alpha_{\text{exp}}^{55}$ |
|-----|---------------|----------------------|------------------|------------------|-----------------|-----------------|-----------------|-----------------|----------------|-----------------------|----------------------------|
| gas | $\alpha_{zz}$ | 12.970               | 0.185            | 0.088            | 1.513           | −0.004          | −0.008          | 0.584           | 202.0          | 217.3                 |                            |
|     | $\alpha_{is}$ | 10.420               | 0.160            | 0.066            | 1.555           | 0.004           | −0.006          | 0.656           | 202.0          | 214.9                 |                            |
| sol | $\alpha_{zz}$ | 17.335               | 0.268            | 0.130            | 2.406           | 0.009           | −0.008          | 1.000           | 300.4          | 321.6                 |                            |
|     | $\alpha_{is}$ | 14.211               | 0.244            | 0.097            | 1.872           | −0.007          | −0.007          | 2.005           | 300.4          | 318.8                 | 330 ± 6                    |

wavelength. The computed values are only slightly different than the static ones, and solvent effects remain very relevant, leading to an increase in the computed polarizability, like in the static case. Vibrational nonequilibrium only causes very slight changes in the computed values, while local field effects, computed in this case using the solvent's optical dielectric constant, significantly affect the electronic part.

From the same paper by Wortmann et al.,<sup>55</sup> we find that the experimental value is  $14.1 \pm 0.4 \text{ cm}^3 \text{ mol}^{-1}$ , which happens to be exactly the same as the total computed value ( $14.08 \text{ cm}^3 \text{ mol}^{-1}$ ), confirming the validity of our methodology.

The second system we studied is 3,5-dinitroaniline (dNA, Figure 1b) in the gas phase and 1,4-dioxane solution. dNA has a similar structure to pNA and analogous push–pull properties. As in the case of pNA, the equilibrium structure of dNA in both the gas phase and in solution is predicted to be nonplanar because of the pyramidalized aminic group. As for pNA, we perform all calculations on the molecule optimized with a  $C_{2v}$  geometry and discard the mode with imaginary frequency in the calculation of the pure vibrational components of the polarizability and of the vibrational averaging.

Table 3 reports all the contributions to the longitudinal (along the molecular axis) and isotropic static polarizability. The vibrational correction  $\Delta_{\text{ZP}}\alpha$  to the isotropic polarizability is about 2% of the corresponding electronic value, with the greatest contribution coming from  $[\alpha]^{1,0}$ , which accounts for the electric anharmonicity of the electronic polarizability. An opposite conclusion can be reached in the case of the pure vibrational component, whose most important term is  $[\mu^2]^{0,2}$ , which is entirely due to the anharmonicity of the PES. This is not surprising as the pure vibrational component is computed from the electric dipole derivatives rather than the polarizability derivatives, and the former may have a less pronounced dependence on the molecular geometry compared to the latter. In addition, the vibrational correction  $[\alpha]^{0,1}$  depends on the mechanical anharmonicity only through the semidiagonal cubic force constants  $K_{abb}$ , whereas the pure vibrational component  $[\mu^2]^{0,2}$  requires all third derivatives as well as the semidiagonal fourth derivatives of the electronic energy (the complete expression of the  $[\mu^2]^{0,2}$  term can be found in the Appendix). Introducing solvent effects has a dramatic effect on all quantities, with a 40% increase in the electronic isotropic value and the vibrational correction, and an even greater effect on the pure vibrational part, which becomes very considerable with respect to the electronic polarizability, highlighting the usefulness of including both vibrational and environmental effects in a coherent manner.

Table 4 reports the electronic and vibrational corrections to the dynamic polarizability computed at the sodium-D wavelength (589 nm). We only show the vibrational correction in this case because the pure vibrational term is negligibly small for this wavelength. The results for the dynamic polarizability mirror the static ones: solvent effects produce an increase in both the electronic polarizability and the vibrational correc-

Table 4. Dynamic Polarizability of dNA in Vacuo and 1,4-Dioxane Solution Computed for a 589 nm Wavelength

|     |               | $\alpha^{\text{eq}}$ | $[\alpha]^{1,0}_{\omega}$ | $[\alpha]^{0,1}_{\omega}$ | $\alpha_{\text{tot}}$ | $\alpha_{\text{exp}}^{55}$ |
|-----|---------------|----------------------|---------------------------|---------------------------|-----------------------|----------------------------|
| gas | $\alpha_{zz}$ | 13.75                | 0.23                      | 0.10                      | 14.08                 |                            |
|     | $\alpha_{is}$ | 11.07                | 0.21                      | 0.07                      | 11.35                 |                            |
| sol | $\alpha_{zz}$ | 18.12                | 0.35                      | 0.15                      | 18.61                 |                            |
|     | $\alpha_{is}$ | 14.88                | 0.32                      | 0.11                      | 15.32                 | 15.5 ± 0.1                 |

tions, and for the latter, the electric anharmonicity is the dominant effect.

The static and dynamic polarizability of dNA in 1,4-dioxane has also been studied experimentally by Wortmann et al.,<sup>55</sup> who obtained values of  $330 \pm 6$  and  $15.5 \pm 0.1 \text{ cm}^3 \text{ mol}^{-1}$  for  $\alpha$  and  $\alpha_{\omega}$ , respectively. The static value includes the orientational contribution discussed above, which we also computed obtaining a value of  $300.4 \text{ cm}^3 \text{ mol}^{-1}$ . By summing all contributions, we obtain total calculated values of 319 and  $15.3 \text{ cm}^3 \text{ mol}^{-1}$  for  $\alpha$  and  $\alpha_{\omega}$ , respectively. The experimental values are very well reproduced in both cases, confirming the validity of our approach.

The next system we analyze is 2,6-di-*n*-propyl-4*H*-pyran-4-ylidenemalononitrile (DPDCP), shown in Figure 1c, in  $\text{CCl}_4$  solution. In this case we only limit ourselves to the dynamic polarizability computed at 633 nm, for which experimental measurements exist.<sup>56</sup> Results are summarized in Table 5. The

Table 5. Dynamic Polarizability of DPDCP in  $\text{CCl}_4$  Solution Computed for a 633 nm Wavelength

|               |               | $\alpha^{\text{eq}}$ | $[\alpha]^{1,0}_{\omega}$ | $[\alpha]^{0,1}_{\omega}$ | $\alpha_{\text{tot}}$ | $\alpha_{\text{exp}}^{56}$ |
|---------------|---------------|----------------------|---------------------------|---------------------------|-----------------------|----------------------------|
| $\alpha_{zz}$ |               | 33.70                | 1.64                      | 0.01                      | 35.35                 |                            |
|               | $\alpha_{is}$ | 23.67                | 1.36                      | 0.01                      | 25.04                 | 27.3                       |

discussion is very similar as in the two previous cases: the electric anharmonicity gives again the greatest contribution to the zero-point polarizability, whose inclusion shifts the computed value in the right direction with respect to the experimental measurement.

**4.1. Bichromophoric System.** After testing the method, we moved to the larger system shown in Figure 3 (1,4-bis(4'-dimethylamino-3',5'-dicyanophenyl)bicyclo[2,2,2]octane) in benzene solution. The molecule is composed of two aromatic chromophores bridged by an aliphatic bicyclooctane structure. We computed the static and dynamic polarizability of the system as a whole (A), and of the chromophore (B) and bridging structure (C) alone, to test whether the polarizability of the whole structure might be the sum of the three independent terms. Table 6 shows both the static and dynamic electronic polarizabilities of the molecule (the latter computed at a 1086 nm wavelength), as well as the respective harmonic pure vibrational contributions.

In the case of the static polarizability, the harmonic pure vibrational contribution represents about 8% of the electronic value, whereas its dynamic counterpart appears to be negligible, for both the whole molecule and its structural building blocks.

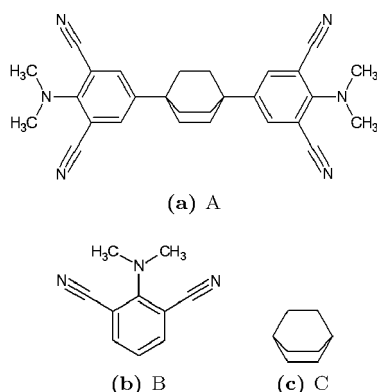


**Figure 3.** Structure of the bichromophoric system and its constituent parts studied.

**Table 6.** Static and Dynamic Polarizability of the Bichromophoric System in Benzene Solution

|      |                      | $\alpha^{\text{eq}}$ | $[\mu^2]^{0,0}$ | $\alpha_{\text{av}}^{\text{eq}}$ | $[\mu^2]_{\text{av}}^{0,0}$ |
|------|----------------------|----------------------|-----------------|----------------------------------|-----------------------------|
| A    | $\alpha_{zz}$        | 52.55                | 4.25            | 53.67                            | −0.08                       |
|      | $\alpha_{\text{is}}$ | 43.97                | 3.34            | 44.64                            | −0.04                       |
| B    | $\alpha_{zz}$        | 20.62                | 1.29            | 20.83                            | −0.01                       |
|      | $\alpha_{\text{is}}$ | 16.31                | 2.00            | 16.60                            | −0.02                       |
| C    | $\alpha_{zz}$        | 10.17                | 0.12            | 10.22                            | −0.01                       |
|      | $\alpha_{\text{is}}$ | 10.17                | 0.11            | 10.22                            | −0.01                       |
| 2B+C | $\alpha_{zz}$        | 51.41                | 2.70            | 51.88                            | −0.03                       |
|      | $\alpha_{\text{is}}$ | 42.79                | 4.11            | 43.42                            | −0.05                       |

The results also suggest that the purely electronic polarizability can be safely computed by summing the contributions three separate pieces (2B + C). The total electronic polarizability obtained this way has only a 3% error with respect to the one computed for the whole system. This is not surprising as molecular polarizabilities can sometimes be estimated by summing atomic and/or functional group contributions.<sup>57</sup> Unfortunately, the same cannot be said for the pure vibrational polarizability: the values obtained for the A structure differ significantly from the 2B + C ones. This is expected as the vibrational modes of the whole molecule tend to be highly delocalized and, owing to its  $C_2$  symmetry, they often appear as symmetric and antisymmetric combinations of local vibrations.

The dynamic polarizability of molecule A in benzene has been measured by Liptay et al.,<sup>58</sup> who report a value of  $560 \pm 6 \text{ cm}^3 \text{ mol}^{-1}$ . This is 1 order of magnitude greater than the value we computed. Given the accuracy of the results obtained for the other systems described here with respect to their experimental counterparts we believe this discrepancy may be due to an error in the experimental measurement. This result may stimulate new experimental studies on this system.

## 5. CONCLUSIONS AND PERSPECTIVES

We have presented a methodology for computing static and frequency-dependent polarizabilities of molecular systems in the condensed phase that takes into account both vibrational and electronic effects. All contributions to the computed polarizability, i.e., the orientational component, the purely electronic contribution, and the zero-point and pure vibrational corrections, were computed with the inclusion of solvent effects modeled via PCM. Vibrational effects were computed using an anharmonic PES via perturbation theory, and the geometrical dependence of the electronic properties under consideration,

be it the polarizability or the dipole moment, were also taken into account by means of Taylor expansions truncated at the appropriate order. We took particular care when including electronic and/or vibrational nonequilibrium effects on the different terms that constitute the computed physical quantity, so the purely electronic component and its zero-point correction were calculated under the electronic nonequilibrium solvation regime, while vibrational nonequilibrium effects were included in the latter and in the pure vibrational polarizability, both at the harmonic and anharmonic levels. Local field effects were also included in all contributions,<sup>8</sup> as it has been shown that they may lead to substantial changes to the computed values. The ability of this model to introduce nonspecific solvent effects on all components of the computed polarizability should discourage the use of the popular, albeit very approximate, Onsager–Lorentz model to estimate the cavity field and reaction field factors and obtain the gas-phase value from its solution one and vice versa. Specific solvation effects can be easily introduced by adding explicit solvent molecules to the portion of the system treated quantum-mechanically, or through mixed quantum-mechanical/classical models such as the QM/FQ/PCM model we have recently implemented.<sup>59–61</sup> This model provides a consistent description of the electronic properties of molecular systems in solution and yields computed values that can be directly compared with experimental measurements, as exemplified by the accuracy of the computed values presented here. We believe these results show that while the use of more accurate (and expensive) electronic structure methods in conjunction with larger basis sets can surely increase the accuracy of the purely electronic component, this should not come at the cost of forsaking the other contributions.

## APPENDIX

We used the following expression for the  $[\mu^2]^{0,2}$  term in the pure vibrational polarizability (i.e., the one due to the mechanical anharmonicity only):

$$\begin{aligned}
 [\mu^2]^{0,2} = & -\frac{\hbar}{8} \sum_{\alpha\beta} \hat{p}_{\alpha\beta} \sum_{ab} \frac{1}{\omega_a} \left\{ \frac{1}{2} F_{aabb} \frac{\partial \mu_\alpha}{\partial Q_b} \frac{\partial \mu_\beta}{\partial Q_b} \frac{\lambda_b}{\omega_b^2} \right. \\
 & + \sum_{c \neq b} F_{aabc} \frac{\partial \mu_\alpha}{\partial Q_b} \frac{\partial \mu_\beta}{\partial Q_c} \lambda_b \lambda_c + \\
 & - \sum_c \left[ \frac{1}{2} F_{aabb} F_{bcc} \frac{\partial \mu_\alpha}{\partial Q_c} \frac{\partial \mu_\beta}{\partial Q_c} \frac{\lambda_c}{\omega_b^2 \omega_c^2} \right. \\
 & + F_{abc} F_{abc} \frac{\partial \mu_\alpha}{\partial Q_c} \frac{\partial \mu_\beta}{\partial Q_c} \lambda_{ab} \lambda_c \frac{(\omega_a + \omega_b)^2 - 2\omega_c^2 - \omega^2}{(\omega_a + \omega_b)^2 - \omega_c^2} \\
 & + + \sum_{d \neq c} \left( F_{aabb} F_{bcd} \frac{\partial \mu_\alpha}{\partial Q_c} \frac{\partial \mu_\beta}{\partial Q_d} \frac{\lambda_c \lambda_d}{\omega_b^2} \right. \\
 & \left. \left. + 2F_{abc} F_{abd} \frac{\partial \mu_\alpha}{\partial Q_c} \frac{\partial \mu_\beta}{\partial Q_d} \lambda_{ab} \lambda_c \lambda_d \right) \right\}
 \end{aligned}$$

where  $F_{abc}$  and  $F_{abcd}$  are the cubic and quartic force constants,  $\omega_a$  denotes the angular harmonic frequency of normal mode  $a$ ,  $\omega$  is the angular frequency of the applied electric field, and the operator  $\sum_{\alpha\beta} \hat{p}_{\alpha\beta}$  permutes the two dipole components ( $\sum_{\alpha\beta} \hat{p}_{\alpha\beta} f(\mu_\omega, \mu_\beta) = f(\mu_\omega, \mu_\beta) + f(\mu_\omega, \mu_\beta)$ ). We also use the



quantities  $\lambda_{ab} = ((\omega_a + \omega_b)^2 - \omega^2)^{-1}$  and  $\lambda_c = (\omega_c^2 - \omega^2)^{-1}$ . All derivatives are understood to be performed with respect to the mass-weighted normal modes at the equilibrium geometry.

## ■ ASSOCIATED CONTENT

### ● Supporting Information

Electronic static and dynamic (computed at 589 nm) polarizabilities (in  $\text{cm}^3 \text{mol}^{-1}$ ) of para-nitroaniline (pNA) in vacuo and 1,4-dioxane, computed with different functionals with the aug-cc-pVDZ basis set. Electronic and harmonic pure vibrational static and dynamic (at 589 nm wavelength, and denoted by a subscript  $\omega$ ) polarizability of pNA in acetonitrile. Graphical representation of the normal modes of pNA in the gas phase, obtained at the CAM-B3LYP/aug-cc-pVDZ level of theory. This material is available free of charge via the Internet at <http://pubs.acs.org>.

## ■ AUTHOR INFORMATION

### Corresponding Author

\*E-mail: [franco.egidi@sns.it](mailto:franco.egidi@sns.it).

### Notes

The authors declare no competing financial interest.

## ■ ACKNOWLEDGMENTS

Franco Egidi gratefully acknowledges support from COST (Action CoDECS: “CONvergent Distributed Environment for Computational Spectroscopy”). Vincenzo Barone would like to acknowledge the ERC project (European Research Council Advanced Grant 320951-DREAMS). Chiara Cappelli acknowledges support from the Italian MIUR PRIN 2012 NB3KLK\_002, and Julien Bloino would also like to acknowledge support from the Italian MIUR (FIRB 2012: Progettazione di materiali nanoeterogenei per la conversione di energia solare, protocollo: RBFR122HFZ).

## ■ REFERENCES

- (1) Dalton, L. *Polymers for Photonics Applications I*; Springer: New York, 2002; Vol. 7, pp 1–86.
- (2) Kanis, D. R.; Ratner, M. A.; Marks, T. J. Design and construction of molecular assemblies with large second-order optical nonlinearities. Quantum chemical aspects. *Chem. Rev.* **1994**, *94a*, 195–242.
- (3) Verbiest, T.; Houbrechts, S.; Kauranen, M.; Clays, K.; Persoons, A. Second-order nonlinear optical materials: recent advances in chromophore design. *J. Mater. Chem.* **1997**, *7*, 2175–2189.
- (4) Limacher, P. A.; Mikkelsen, K. V.; Lüthi, H. P. On the accurate calculation of polarizabilities and second hyperpolarizabilities of polyacetylene oligomer chains using the CAM-B3LYP density functional. *J. Chem. Phys.* **2009**, *130*, 194114.
- (5) Bishop, D. M. Molecular vibrational and rotational motion in static and dynamic electric fields. *Rev. Mod. Phys.* **1990**, *62*, 343–374.
- (6) Bishop, D. M.; Champagne, B.; Kirtman, B. Relationship between static vibrational and electronic hyperpolarizabilities of  $\pi$ -conjugated push-pull molecules within the two-state valence-bond charge-transfer model. *J. Chem. Phys.* **1998**, *109*, 9987–9994.
- (7) Bishop, D. M.; Champagne, B.; Kirtman, B. Static and dynamic polarizabilities and first hyperpolarizabilities for  $\text{CH}_4$ ,  $\text{CF}_4$ , and  $\text{CCl}_4$ . *J. Chem. Phys.* **1998**, *109*, 8407–8415.
- (8) Cammi, R.; Mennucci, B.; Tomasi, J. An Attempt To Bridge the Gap between Computation and Experiment for Nonlinear Optical Properties: Macroscopic Susceptibilities in Solution. *J. Phys. Chem. A* **2000**, *104*, 4690–4698.
- (9) Barone, V.; Baiardi, A.; Biczysko, M.; Bloino, J.; Cappelli, C.; Lipparini, F. Implementation and validation of a multi-purpose virtual spectrometer for large systems in complex environments. *Phys. Chem. Chem. Phys.* **2012**, *14*, 12404–12422.
- (10) Bloino, J.; Barone, V. A second-order perturbation theory route to vibrational averages and transition properties of molecules: General formulation and application to infrared and vibrational circular dichroism spectroscopies. *J. Chem. Phys.* **2012**, *136*, 124108.
- (11) Egidi, F.; Bloino, J.; Cappelli, C.; Barone, V.; Tomasi, J. Tuning of NMR and EPR parameters by vibrational averaging and environmental effects: an integrated computational approach. *Mol. Phys.* **2013**, *111*, 1345–1354.
- (12) Egidi, F.; Bloino, J.; Barone, V.; Cappelli, C. Toward an Accurate Modeling of Optical Rotation for Solvated Systems: Anharmonic Vibrational Contributions Coupled to the Polarizable Continuum Model. *J. Chem. Theory Comput.* **2012**, *8*, 585–597.
- (13) Helgaker, T.; Coriani, S.; Jorgensen, P.; Kristensen, K.; Olsen, J.; Ruud, K. Recent Advances in Wave Function-Based Methods of Molecular-Property Calculations. *Chem. Rev.* **2012**, *112*, 543–631.
- (14) Bishop, D. M.; Norman, P. In *Handbook of Advanced Electronic and Photonic Materials and Devices*; Nalwa, H. S., Ed.; Academic Press: Waltham, MA, 2001; pp 1–62.
- (15) Bishop, D. M.; Kirtman, B. A perturbation method for calculating vibrational dynamic dipole polarizabilities and hyperpolarizabilities. *J. Chem. Phys.* **1991**, *95*, 2646–2658.
- (16) Bishop, D. M.; Kirtman, B. Compact formulas for vibrational dynamic dipole polarizabilities and hyperpolarizabilities. *J. Chem. Phys.* **1992**, *97*, 5255–5256.
- (17) Liptay, W.; Becker, J.; Wehning, D.; Lang, W.; Burkhard, O. The Determination of Molecular Quantities from Measurements on Macroscopic Systems. II. The Determination of Electric Dipole Moments. *Z. Naturforsch.* **1982**, *37a*, 1396–1408.
- (18) Barone, V. Accurate Vibrational Spectra of Large Molecules by Density Functional Computations beyond the Harmonic Approximation: The Case of Azabenzenes. *J. Phys. Chem. A* **2004**, *108*, 4146–4150.
- (19) Barone, V. Anharmonic vibrational properties by a fully automated second-order perturbative approach. *J. Chem. Phys.* **2005**, *122*, 014108.
- (20) Barone, V.; Bloino, J.; Guido, C. A.; Lipparini, F. A fully automated implementation of VPT2 Infrared intensities. *Chem. Phys. Lett.* **2010**, *496*, 157–161.
- (21) Bloino, J.; Biczysko, M.; Barone, V. General Perturbative Approach for Spectroscopy, Thermodynamics, and Kinetics: Methodological Background and Benchmark Studies. *J. Chem. Theory Comput.* **2012**, *8*, 1015–1036.
- (22) Wortmann, R.; Bishop, D. M. Effective polarizabilities and local field corrections for nonlinear optical experiments in condensed media. *J. Chem. Phys.* **1998**, *108*, 1001–1007.
- (23) Cammi, R. *Molecular Response Functions for the Polarizable Continuum Model*; Springer: New York, 2013.
- (24) Onsager, L. Electric Moments of Molecules in Liquids. *J. Am. Chem. Soc.* **1936**, *58*, 1486–1493.
- (25) Tomasi, J.; Mennucci, B.; Cammi, R. Quantum Mechanical Continuum Solvation Models. *Chem. Rev.* **2005**, *105*, 2999–3093.
- (26) Mennucci, B. Polarizable Continuum Model. *WIREs Comput. Mol. Sci.* **2012**, *2*, 386–404.
- (27) Cappelli, C. In *Continuum Solvation Models in Chemical Physics*; Cammi, R.; Mennucci, B., Eds.; John Wiley & Sons Inc.: Chichester, U. K., 2012; pp 167–179.
- (28) Orr, B. J.; Ward, J. F. Perturbation theory of the non-linear optical polarization of an isolated system. *Mol. Phys.* **1971**, *20*, 513–526.
- (29) Pipolo, S.; Corni, S.; Cammi, R. The cavity electromagnetic field within the polarizable continuum model of solvation. *J. Chem. Phys.* **2014**, *140*, 164114.
- (30) Mennucci, B.; Cammi, R.; Tomasi, J. Excited states and solvatochromic shifts within a nonequilibrium solvation approach. *J. Chem. Phys.* **1998**, *109*, 2798–2807.
- (31) Thicoipe, S.; Carbonniere, P.; Pouchan, C. Comparison of static and dynamic methods of treatment of anharmonicity for the vibrational study of isolated and aqueous forms of guanine. *Chem. Phys. Lett.* **2014**, *591*, 243–247.



- (32) Cappelli, C.; Monti, S.; Scalmani, G.; Barone, V. On the Calculation of Vibrational Frequencies for Molecules in Solution Beyond the Harmonic Approximation. *J. Chem. Theory Comput.* **2010**, *6*, 1660–1669.
- (33) Cappelli, C.; Lipparini, F.; Bloino, J.; Barone, V. Towards an accurate description of anharmonic infrared spectra in solution within the polarizable continuum model: Reaction field, cavity field and nonequilibrium effects. *J. Chem. Phys.* **2011**, *135*, 104505.
- (34) Cappelli, C.; Bloino, J.; Lipparini, F.; Barone, V. Towards Ab-Initio Anharmonic Vibrational circular dichroism spectra in the condensed phase. *J. Phys. Chem. Lett.* **2012**, *3*, 1766–1773.
- (35) Frisch, M. J.; Trucks, G. W.; Schlegel, H. B.; Scuseria, G. E.; Robb, M. A.; Cheeseman, J. R.; Scalmani, G.; Barone, V.; Mennucci, B.; Petersson, G. A.; Nakatsuji, H.; Caricato, M.; Li, X.; Hratchian, H. P.; Izmaylov, A. F.; Bloino, J.; Zheng, G.; Sonnenberg, J. L.; Hada, M.; Ehara, M.; Toyota, K.; Fukuda, R.; Hasegawa, J.; Ishida, M.; Nakajima, T.; Honda, Y.; Kitao, O.; Nakai, H.; Vreven, T.; Montgomery, J. A., Jr.; Peralta, J. E.; Ogliaro, F.; Bearpark, M.; Heyd, J. J.; Brothers, E.; Kudin, K. N.; Staroverov, V. N.; Kobayashi, R.; Normand, J.; Raghavachari, K.; Rendell, A.; Burant, J. C.; Iyengar, S. S.; Tomasi, J.; Cossi, M.; Rega, N.; Millam, J. M.; Klene, M.; Knox, J. E.; Cross, J. B.; Bakken, V.; Adamo, C.; Jaramillo, J.; Gomperts, R.; Stratmann, R. E.; Yazyev, O.; Austin, A. J.; Cammi, R.; Pomelli, C.; Ochterski, J. W.; Martin, R. L.; Morokuma, K.; Zakrzewski, V. G.; Voth, G. A.; Salvador, P.; Dannenberg, J. J.; Dapprich, S.; Daniels, A. D.; Farkas, Ö.; Foresman, J. B.; Ortiz, J. V.; Cioslowski, J.; Fox, D. J. *Gaussian 09*, Revision D.01; Gaussian Inc.: Wallingford, CT, 2009.
- (36) Yanai, T.; Tew, D. P.; Handy, N. C. A new hybrid exchange-correlation functional using the Coulomb-attenuating method (CAM-B3LYP). *Chem. Phys. Lett.* **2004**, *393*, 51–57.
- (37) Bulik, I. W.; Zaleśny, R.; Bartkowiak, W.; Luis, J. M.; Kirtman, B.; Scuseria, G. E.; Avramopoulos, A.; Reis, H.; Papadopoulos, M. G. Performance of density functional theory in computing nonresonant vibrational (hyper)polarizabilities. *J. Comput. Chem.* **2013**, *34*, 1775–1784.
- (38) Baranowska-Łączkowska, A.; Bartkowiak, W.; Góra, R. W.; Pawłowski, F.; Zaleśny, R. On the performance of long-range-corrected density functional theory and reduced-size polarized LPol-n basis sets in computations of electric dipole (hyper)polarizabilities of  $\pi$ -conjugated molecules. *J. Comput. Chem.* **2013**, *34*, 819–826.
- (39) Becke, A. D. Density-functional thermochemistry. III. The role of exact exchange. *J. Chem. Phys.* **1993**, *98*, 5648–5652.
- (40) Lee, C.; Yang, W.; Parr, R. G. Development of the Colle-Salvetti correlation-energy formula into a functional of the electron density. *Phys. Rev. B* **1988**, *37*, 785–789.
- (41) Zhao, Y.; Truhlar, D. G. The M06 suite of density functionals for main group thermochemistry, thermochemical kinetics, non-covalent interactions, excited states, and transition elements: two new functionals and systematic testing of four M06-class functionals and 12 other functionals. *Theor. Chem. Acc.* **2008**, *393*, 215–241.
- (42) Adamo, C.; Barone, V. Toward reliable density functional methods without adjustable parameters: The PBE0 model. *J. Chem. Phys.* **1999**, *110*, 6158–6169.
- (43) Chai, J.-D.; Head-Gordon, M. Systematic optimization of long-range corrected hybrid density functionals. *J. Chem. Phys.* **2008**, *128*, 084106.
- (44) Kendall, R. A.; Dunning, T. H., Jr.; Harrison, R. J. Electron affinities of the first-row atoms revisited. Systematic basis sets and wave functions. *J. Chem. Phys.* **1992**, *96*, 6796–6806.
- (45) Daniel, C.; Dupuis, M. Nonlinear optical properties of organic solids: ab initio polarizability and hyperpolarizabilities of nitroaniline derivatives. *Chem. Lett.* **1990**, *171*, 209–216.
- (46) Karna, S. P.; Prasad, P. N.; Dupuis, M. Nonlinear optical properties of p-nitroaniline: An ab initio time-dependent coupled perturbed Hartree-Fock study. *J. Chem. Phys.* **1991**, *94*, 1171.
- (47) Sim, F.; Chin, S.; Dupuis, M.; Rice, J. E. Electron correlation effects in hyperpolarizabilities of p-nitroaniline. *J. Phys. Chem.* **1993**, *97*, 1158–1163.
- (48) Champagne, B. Vibrational polarizability and hyperpolarizability of p-nitroaniline. *Chem. Phys. Lett.* **1996**, *261*, 57–65.
- (49) Cammi, R.; Frediani, L.; Mennucci, B.; Ruud, K. Multi-configurational self-consistent field linear response for the polarizable continuum model: Theory and application to ground and excited-state polarizabilities of para-nitroaniline in solution. *J. Chem. Phys.* **2003**, *119*, 5818–5827.
- (50) Soscún, H.; Castellano, O.; Bermúdez, Y.; Toro, C.; Cubillán, N.; Hinchliffe, A.; Phu, X. N. B3LYP study of the dipole moment and the static dipole (hyper) polarizabilities of para-nitroaniline in gas phase. *Int. J. Quantum Chem.* **2006**, *106*, 1130–1137.
- (51) Cheng, L. T.; Tam, W.; Stevenson, S. H.; Meredith, G. R.; Rikken, G.; Marder, S. R. Experimental investigations of organic molecular nonlinear optical polarizabilities. I. Methods and results on benzene and stilbene derivatives. *J. Phys. Chem.* **1991**, *95*, 10631–10643.
- (52) Luis, J. M.; Reis, H.; Papadopoulos, M.; Kirtman, B. Treatment of nonlinear optical properties due to large amplitude anharmonic vibrational motions: Umbrella motion in  $\text{NH}_3$ . *J. Chem. Phys.* **2009**, *131*, 034116.
- (53) García-Borràs, M.; Sola, M.; Lauvergnat, D.; Reis, H.; Luis, J. M.; Kirtman, B. A Full Dimensionality Approach to Evaluate the Nonlinear Optical Properties of Molecules with Large Amplitude Anharmonic Tunneling Motions. *J. Chem. Theory Comput.* **2013**, *9*, 520–532.
- (54) Reis, H.; Luis, J. M.; García-Borràs, M.; Kirtman, B. Computation of Nonlinear Optical Properties of Molecules with Large Amplitude Anharmonic Motions. III. Arbitrary Double-Well Potentials. *J. Chem. Theory Comput.* **2014**, *10*, 236–242.
- (55) Wortmann, R.; Krämer, P.; Glania, C.; Lebus, S.; Detzer, N. Deviations from Kleinman symmetry of the second-order polarizability tensor in molecules with low-lying perpendicular electronic bands. *Chem. Phys.* **1993**, *173*, 99–108.
- (56) Wortmann, R.; Poga, C.; Twieg, R. J.; Geletneky, C.; Moylan, C. R.; Lundquist, P. M.; DeVoe, R. G.; Cotts, P. M.; Horn, H.; Rice, J. E.; Burland, D. M. Design of optimized photorefractive polymers: A novel class of chromophores. *J. Chem. Phys.* **1996**, *105*, 10637–10647.
- (57) Kang, Y. K.; Jhon, M. S. Additivity of atomic static polarizabilities and dispersion coefficients. *Theor. Chim. Acta* **1982**, *61*, 41–48.
- (58) Liptay, W.; Wortmann, R.; Schaffrin, H.; Burkhard, O.; Reiting, W.; Detzer, N. Excited State Dipole Moments and Polarizabilities of Centrosymmetric and Dimeric Molecules. I. Model Study of a Bichromophoric Molecule. *Chem. Phys.* **1988**, *120*, 429–438.
- (59) Lipparini, F.; Barone, V. Polarizable Force Fields and Polarizable Continuum Model: A Fluctuating Charges/PCM Approach. I. Theory and Implementation. *J. Chem. Theory Comput.* **2011**, *7*, 3711–3724.
- (60) Lipparini, F.; Cappelli, C.; Barone, V. Linear Response Theory and Electronic Transition Energies for a Fully Polarizable QM/Classical Hamiltonian. *J. Chem. Theory Comput.* **2012**, *8*, 4153–4165.
- (61) Lipparini, F.; Cappelli, C.; Scalmani, G.; De Mitri, N.; Barone, V. Analytical First and Second Derivatives for a Fully Polarizable QM/Classical Hamiltonian. *J. Chem. Theory Comput.* **2012**, *8*, 4270–4278.